



A LETTERS JOURNAL EXPLORING
THE FRONTIERS OF PHYSICS

OFFPRINT

Validity and failure of the Boltzmann weight

L. J. L. CIRTO, A. RODRÍGUEZ, F. D. NOBRE and C. TSALLIS

EPL, **123** (2018) 30003

Please visit the website
www.epljournal.org

Note that the author(s) has the following rights:

- immediately after publication, to use all or part of the article without revision or modification, **including the EPLA-formatted version**, for personal compilations and use only;
- no sooner than 12 months from the date of first publication, to include the accepted manuscript (all or part), **but not the EPLA-formatted version**, on institute repositories or third-party websites provided a link to the online EPL abstract or EPL homepage is included.

For complete copyright details see: <https://authors.eplletters.net/documents/copyright.pdf>.



epl

A LETTERS JOURNAL EXPLORING
THE FRONTIERS OF PHYSICS

AN INVITATION TO SUBMIT YOUR WORK

epljournal.org

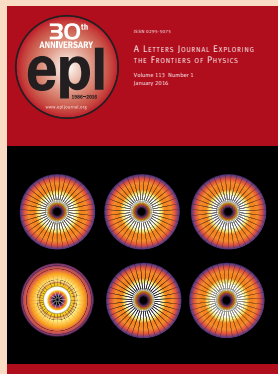
The Editorial Board invites you to submit your letters to EPL

EPL is a leading international journal publishing original, innovative Letters in all areas of physics, ranging from condensed matter topics and interdisciplinary research to astrophysics, geophysics, plasma and fusion sciences, including those with application potential.

The high profile of the journal combined with the excellent scientific quality of the articles ensures that EPL is an essential resource for its worldwide audience. EPL offers authors global visibility and a great opportunity to share their work with others across the whole of the physics community.

Run by active scientists, for scientists

EPL is reviewed by scientists for scientists, to serve and support the international scientific community. The Editorial Board is a team of active research scientists with an expert understanding of the needs of both authors and researchers.



epljournal.org

OVER

568,000

full text downloads in 2015

18 DAYS

average accept to online
publication in 2015

20,300

citations in 2015

*"We greatly appreciate
the efficient, professional
and rapid processing of
our paper by your team."*

Cong Lin
Shanghai University

Six good reasons to publish with EPL

We want to work with you to gain recognition for your research through worldwide visibility and high citations. As an EPL author, you will benefit from:

- 1 Quality** – The 60+ Co-editors, who are experts in their field, oversee the entire peer-review process, from selection of the referees to making all final acceptance decisions.
- 2 Convenience** – Easy to access compilations of recent articles in specific narrow fields available on the website.
- 3 Speed of processing** – We aim to provide you with a quick and efficient service; the median time from submission to online publication is under 100 days.
- 4 High visibility** – Strong promotion and visibility through material available at over 300 events annually, distributed via e-mail, and targeted mailshot newsletters.
- 5 International reach** – Over 3200 institutions have access to EPL, enabling your work to be read by your peers in 100 countries.
- 6 Open access** – Articles are offered open access for a one-off author payment; green open access on all others with a 12-month embargo.

Details on preparing, submitting and tracking the progress of your manuscript from submission to acceptance are available on the EPL submission website epletters.net.

If you would like further information about our author service or EPL in general, please visit epijournal.org or e-mail us at info@epijournal.org.

EPL is published in partnership with:



European Physical Society



Società Italiana
di Fisica

Società Italiana di Fisica



EDP Sciences

IOP Publishing

IOP Publishing

Validity and failure of the Boltzmann weight

L. J. L. CIRTO¹, A. RODRÍGUEZ², F. D. NOBRE^{1,3} and C. TSALLIS^{1,3,4,5}

¹ Centro Brasileiro de Pesquisas Físicas - Rua Dr. Xavier Sigaud 150, 22290-180 Rio de Janeiro, Brazil

² Departamento de Matemática Aplicada a la Ingeniería Aeroespacial, Universidad Politécnica de Madrid Plaza Cardenal Cisneros s/n, 28040 Madrid, Spain

³ National Institute of Science and Technology for Complex Systems - Rua Dr. Xavier Sigaud 150, 22290-180 Rio de Janeiro, Brazil

⁴ Santa Fe Institute - 1399 Hyde Park Road, Santa Fe, 87501 NM, United States

⁵ Complexity Science Hub Vienna - Josefstädter Strasse 39, 1080 Vienna, Austria

received 11 April 2018; accepted in final form 2 August 2018

published online 24 August 2018

PACS 05.45.-a – Nonlinear dynamics and chaos

PACS 05.40.Fb – Random walks and Levy flights

PACS 05.70.Ce – Thermodynamic functions and equations of state

Abstract – The dynamics and thermostatics of a classical inertial XY model, characterized by long-range interactions, are investigated on d -dimensional lattices ($d = 1, 2$, and 3), through molecular dynamics. The interactions between rotators decay with the distance r_{ij} like $1/r_{ij}^\alpha$ ($\alpha \geq 0$), where $\alpha \rightarrow \infty$ and $\alpha = 0$ respectively correspond to the nearest-neighbor and infinite-range interactions. We verify that the momenta probability distributions are Maxwellians in the short-range regime, whereas q -Gaussians emerge in the long-range regime. Moreover, in this latter regime, the individual energy probability distributions are characterized by long tails, corresponding to q -exponential functions. The present investigation strongly indicates that, in the long-range regime, central properties fall out of the scope of Boltzmann-Gibbs statistical mechanics, depending on d and α through the ratio α/d .

Copyright © EPLA, 2018

Systems with long-range-interacting elements have been object of many researches and controversies. Usually, these systems are addressed through statistical-mechanical techniques, and they cover from physical, biological, and mathematical models to complex networks [1–21]. Interesting phenomena, like breakdown of ergodicity, nonequivalence of statistical ensembles, and long-lived quasistationary states, emerge frequently when long-range forces come into play; such situations usually fall out of the scope of Boltzmann-Gibbs (BG) statistical mechanics, which has been developed assuming explicitly, or tacitly, short-range interactions between elements.

For N -body Hamiltonian systems in d -dimensions, with a potential $\Phi(r) \propto 1/r^\alpha$, the case $\alpha/d = 1$ represents a threshold between long- and short-range regimes. By considering a model ruled by this power-law dependence, one interpolates between the infinite-range-interaction ($\alpha = 0$) and the nearest-neighbor ($\alpha \rightarrow \infty$) limits, allowing to investigate the influence of the interaction range on the thermostatics of the model. In the long-range regime, corresponding to $0 \leq \alpha \leq d$, the potential energy, as well as the total energy, scale superlinearly with N so that

the system is said to be nonextensive. In this case, BG statistical mechanics faces several difficulties. In order to derive thermodynamic properties one may redefine the thermodynamic limit [3–6], or employ a properly generalized Kac's prescription, by weakening the strength of interparticle forces as the system size N increases—an artificial modification of the model to turn its total energy extensive. However, even if extensivity is formally recovered by a microscopic modification like Kac's prescription, the system preserves its long-range nature for small values of α . For instance, one may mention the behavior of the Lyapunov exponent [6,7], the presence of non-Boltzmannian quasistationary states (QSSs) [8–10,22], the emergence of typical nonextensive features like q -Gaussians and q -exponentials [10–12], among others. Some of those features remain beyond the threshold $\alpha/d = 1$, where the system can still display long-range properties (see, *e.g.*, ref. [13] and references therein).

A paradigmatic Hamiltonian model, frequently used to investigate several of the above-mentioned properties, is defined in terms of classical XY rotators with infinite-range interactions. In this limit, the BG equilibrium state

is exactly tractable within the standard mean-field approach. Due to this, this model is usually known in the literature as the Hamiltonian-Mean-Field (HMF) one [1,14]. The HMF model has been numerically and analytically studied intensively in the last two decades, and one of its intriguing features concerns the existence of QSSs whose lifetime diverges as the system size N increases. Particularly, these QSSs exhibit a clear breakdown of ergodicity, in the sense that velocity distributions calculated from time averages [15,16] appear to be quite different from those of ensemble averages [1,10,15,16,23–26]. Moreover, for any finite N , the QSSs are followed by a second plateau at longer times, which presents a kinetic temperature that coincides with the one calculated analytically from BG statistical mechanics, although it also exhibits further curious properties, like time-averaged long-tailed velocity distributions [10], in notorious contrast with the BG theory.

Herein we present a numerical analysis of the so-called α -XY model, which consists of a classical XY rotator system, with controllable range of (ferromagnetic) interactions, decaying like $1/r^\alpha$. Previous results ($\alpha = 0$ and $d = 1$) revealed, among other nonstandard features, non-Maxwellian velocity distributions [10,15,16]. In the short-range regime, on the other hand, all the standard BG results are recovered, including, naturally, the Maxwellian distribution. It has been verified that these non-Maxwellian distributions are well fitted along several decades with the so-called q -Gaussians, landmark functions of nonextensive statistical mechanics, built on the basis of the nonadditive entropy S_q [27–29]; similarly, Maxwellians represent a landmark of BG statistics, built from the additive entropy S_{BG} . Indeed, the entropy S_q is defined as a generalization of S_{BG} ,

$$S_q = k \sum_{i=1}^W p_i \ln_q \frac{1}{p_i} \left[\ln_q x \equiv \frac{x^{1-q} - 1}{1-q}; (x > 0) \right], \quad (1)$$

where W accounts for the microscopic configurations, and $\ln_q x$ denotes the q -logarithm; we verify that $S_{BG} \equiv -k \sum p_i \ln p_i = \lim_{q \rightarrow 1} S_q$. The q -exponential $\exp_q[-\beta x] = [1 - \beta(1-q)x]^{1/(1-q)}$ and the q -Gaussian $\exp_q[-\beta x^2]$ appear naturally by extremizing S_q under appropriate constraints [27–29]. The generalized thermostatics based on S_q frequently applies when assumptions underlying the BG thermostatics are not fulfilled (like, *e.g.*, mixing and ergodicity) [10–12,19,20,29–33].

In the present work we are primarily interested on how α/d influences the one-particle velocity and energy distributions of the α -XY model, focusing mainly on the second plateau that follows the QSS at longer times. We explore how higher values of d modify previous $d = 1$ results for the velocity distribution; moreover, we show how the energy distribution changes from the celebrated exponential Boltzmann weight to a distribution well described by a q -exponential, as the system goes from the

short- to the long-range regime. We have also verified a universal scaling law of these distributions governed by the α/d ratio, similarly to what was found in other complex systems [19,20].

We consider the α -XY model on d -dimensional hypercubic lattices, defined by a Hamiltonian, $\mathcal{H} = K + V$ (kinetic and potential contributions, respectively), conveniently written below in terms of one-particle energies E_i ,

$$\mathcal{H} = \sum_{i=1}^N E_i; \quad E_i = \frac{1}{2} p_i^2 + \frac{1}{2\tilde{N}} \sum_{j \neq i}^N \frac{1 - \cos(\theta_i - \theta_j)}{r_{ij}^\alpha}. \quad (2)$$

At a given time t , each rotator i ($i = 1, 2, \dots, N$) is characterized by the angle $\theta_i(t)$ and its conjugated momentum $p_i(t)$, so that the dynamics of the system follows from the Hamilton equations of motion,

$$\dot{\theta}_i = \frac{\partial \mathcal{H}}{\partial p_i} = p_i; \quad \dot{p}_i = -\frac{\partial \mathcal{H}}{\partial \theta_i} = -\frac{1}{\tilde{N}} \sum_{j \neq i}^N \frac{\sin(\theta_i - \theta_j)}{r_{ij}^\alpha}, \quad (3)$$

where $r_{ij} = |\mathbf{r}_i - \mathbf{r}_j|$ measures the distance between rotators at sites i and j in lattice units, and it is defined as the minimal one, given that periodic conditions will be considered. The parameter $\alpha \geq 0$ controls the interaction range, whereas the scaling prefactor $1/\tilde{N}$ in the potential energy of Hamiltonian (2) is introduced to make the energy extensive for all values of α/d , where [3,4,6,17,18]

$$\tilde{N} = \frac{1}{N} \sum_{i=1}^N \sum_{j \neq i}^N \frac{1}{r_{ij}^\alpha} = \sum_{j=2}^N \frac{1}{r_{1j}^\alpha} \quad (\tilde{N} = 2d \text{ for } \alpha \rightarrow \infty), \quad (4)$$

the $0 \leq \alpha/d \leq 1$ ($\alpha/d > 1$) regime being hereafter referred to as long-range (short-range). Notice that when $\alpha = 0$, we get $\tilde{N} = N - 1 \sim N$, so that eq. (2) recovers the HMF model.

The results that follow were obtained from microcanonical molecular-dynamical simulations of a single realization of the system defined in (2), considering fixed values for the number of rotators N and energy per particle u , so that the total energy $E = Nu$ is a constant. To integrate the $2N$ equations of motion in (3), we have used the Yoshida 4th-order symplectic algorithm [34], choosing an integration step in such a way to yield a conservation of the total energy within a relative fluctuation always smaller than 10^{-5} . At the initial time, all rotators were started with $\theta_i = 0$ ($\forall i$); moreover, each momentum p_i was drawn from a symmetric uniform distribution $p_i \in [-1, 1]$, and then rescaled to achieve the desired energy u , as well as zero total angular momentum $P = \sum_i p_i = 0$, which also is a constant of motion. As verified by many authors (see, *e.g.*, refs. [8,10,22]), the model in eq. (2) exhibits a QSS for $0 \leq \alpha/d < 1$ and $u \simeq 0.69$, after which, a crossover to a state whose temperature coincides with the one obtained within BG statistical mechanics [14,18] occurs; herein we explore further properties of this model for the energy $u = 0.69$.

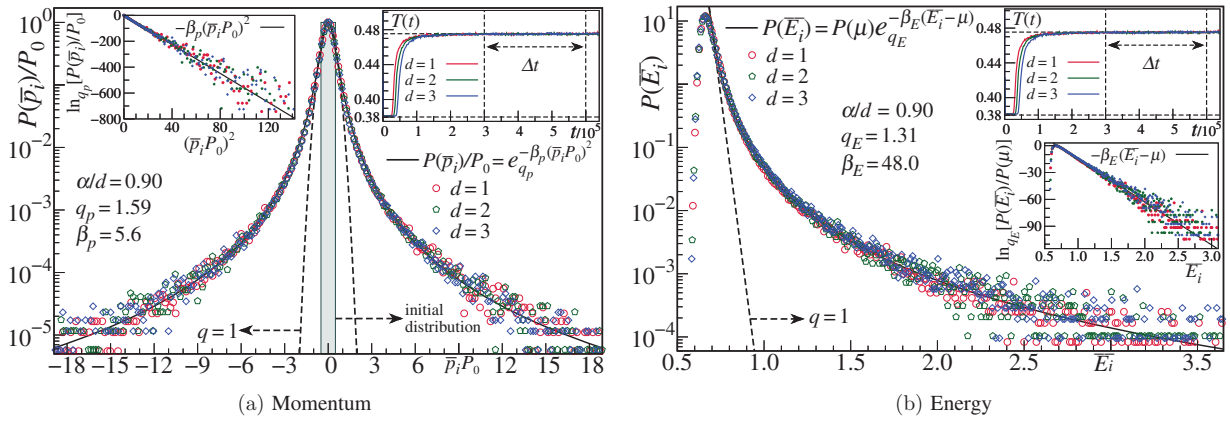


Fig. 1: (Colour online) Distributions of time-averaged momenta \bar{p}_i and energies \bar{E}_i (with $\tau = 1$) for $\alpha/d = 0.9$, in $d = 1, 2$ and 3 dimensions. The simulations were carried for the energy per particle $u = 0.69$ and total number of rotators $N = 1000000$. (a) The distribution $P(\bar{p}_i)$ is shown ($P_0 \equiv P(\bar{p}_i = 0)$); the full line is a q -Gaussian with $q_p = 1.59$ and $\beta_p = 5.6$; the dashed line is a Gaussian ($q = 1$). The left inset shows the same data in a q -logarithm *vs.* squared-momentum representation; a straight line is obtained as expected (since $\ln_q(e_x^x) = x$). (b) The full line represents the q -exponential $P(\bar{E}_i) = P(\mu) \exp_{q_E}[-\beta_E(\bar{E}_i - \mu)]$, with $q_E = 1.31$ ($\beta_E = 48.0$, $\mu = 0.69$, and $P(\mu) = 12$); the corresponding exponential (dashed line) is also shown for comparison. Since the density of states is necessary to reproduce the entire range of data, the parameter μ was introduced in the fitting. The bottom inset shows a straight line by using the q -logarithm in the ordinate. The kinetic temperature $T(t) \equiv 2K(t)/N$, and time window Δt along which the time averages were calculated, coincide in both cases (shown as insets). In all plots one notices the collapse of all dimensions with nearly the same value of q .

In fig. 1 we present results for distributions of momenta (fig. 1(a)) and energies (fig. 1(b)) of the model on hypercubic lattices ($d = 1, 2$ and 3), in the long-range regime, more specifically, $\alpha/d = 0.9$. In the insets on the right-hand sides we show the time evolution of the kinetic temperature $T(t) = 2K(t)/N$, as well as the time interval considered for the histograms. These distributions were calculated by registering n times, *e.g.*, the momenta $p_i(t)$ ($\forall i$), at successive times separated by an interval τ , and then, following the Central Limit Theorem recipe, the arithmetic average $\bar{p}_i = \frac{1}{n} \sum_{k=0}^{n-1} p_i(t_0 + k\tau)$ was obtained, leading to a histogram of these N arithmetic averages. Notice that such a recipe yields precisely a time average in this case (associated with the time window $\Delta t = n\tau$), a situation that frequently corresponds to real experiments. In order to improve the statistics of the histograms, we have considered rather large systems, up to $N = 10^6$, for a single numerical realization in each dimension d . Curiously, although the kinetic temperature coincides with the BG prediction, the momentum distribution is quite distinct from a Gaussian; indeed, due to the long-range nature of the interactions, the resulting distribution exhibits a q -Gaussian form, as already observed in previous $(d, \alpha) = (1, 0)$ works [10,15,16]; fig. 1(a) extends these investigations to higher dimensions. Repeating the foregoing procedure to the one-particle energies $E_i(t)$ (cf. eq. (2)), the distributions in fig. 1(b) are obtained. One sees that a q -Gaussian emerges as the distribution of momenta (instead of a Maxwellian), whereas a q -exponential appears for the energies (instead of the exponential Boltzmann weight). The results of figs. 1(a) and (b) are clearly out of the BG world and in close

agreement with the predictions of q -generalized statistical mechanics.

The histograms shown in figs. 1(a), (b) were obtained from numerical simulations of $N = 10^6$ rotators with $\tau = 1$ (5 integration steps) and $n = 300000$; however, a systematic study for several values of α/d was carried by considering a smaller number of rotators (and consequently, different time windows), due to computational costs. In figs. 2(a), (b) we present the values of q obtained from the distributions of time-averaged momenta \bar{p}_i and energies \bar{E}_i (labeled by q_p and q_E , respectively) *vs.* α/d in $d = 1, 2$ and 3 dimensions. It should be mentioned that the results of fig. 2(a) are in good agreement with previous studies of the $d = 1$ case [10]; here we also investigate $d = 2, 3$. A remarkable collapse is shown (within error bars) as a function of α/d for all dimensions; notice also that, generically, q_p and q_E do not coincide. Intriguingly, these values of q do not attain unit around $\alpha/d = 1$, but rather at some higher value, close to $\alpha/d = 2$. This fact has also been observed in recent simulations of other models with power-law decay of interactions: i) a one-dimensional quantum Ising ferromagnet [35]; ii) a Fermi-Pasta-Ulam-like one-dimensional Hamiltonian with a quartic coupling constant decaying with the distance between oscillators [11,12,36]; iii) scale-free complex networks [19,20]. Similarly to the present investigation, in these previous works three distinct regimes were found, namely, a non-BG long-range interacting regime ($0 \leq \alpha/d \leq 1$), a non-BG short-range one ($1 < \alpha/d \leq a_c$), and the standard BG short-range regime ($\alpha/d > a_c$); for some classical Hamiltonians, $a_c \approx 2$, whereas, for complex networks, $a_c \approx 5$. The existence of these three regimes might be related to ergodicity and

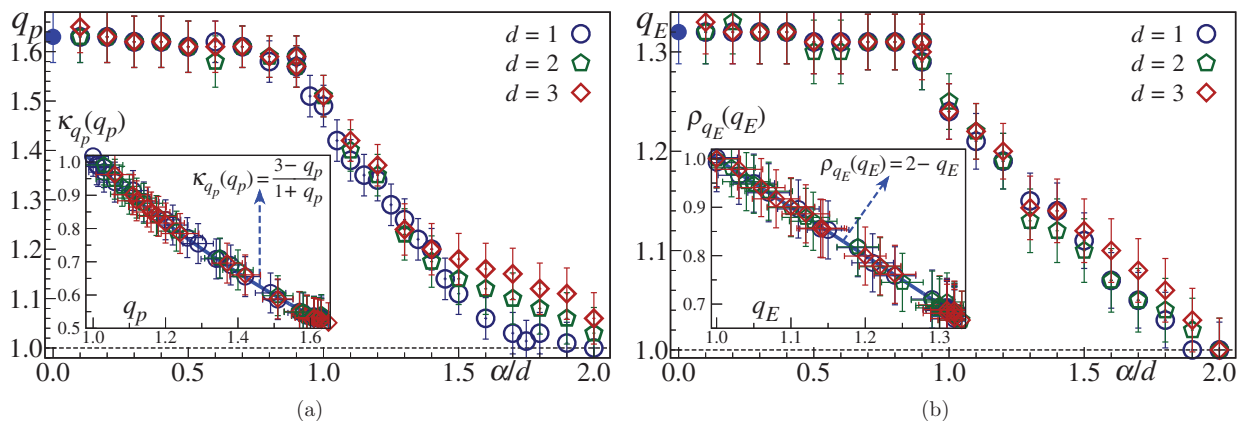


Fig. 2: (Colour online) (α/d) -dependence of the indices q_p and q_E associated respectively with the distributions of time-averaged momenta \bar{p}_i and energies \bar{E}_i for $d = 1, 2, 3$ and $u = 0.69$. The insets show the corresponding q -kurtosis (a) and q -ratio (b), compared to the analytical results (solid curves). The full bullets correspond to the values for $\alpha = 0$. Notice that, within the error bars, the indices q remain constant for $0 \leq \alpha/d \leq 1$, and approach unit only around $\alpha/d = 2$ (see text).

phase-space structure. More precisely, strong indications exist that, for $0 \leq \alpha/d \leq 1$ ($\alpha/d > 1$), weak (strong) chaos emerges [6,7]. How come an intermediate region ($1 < \alpha/d < \alpha_c$) exists, which is ergodic and nevertheless non-BG? A plausible explanation is that, similarly to the web map [37], ergodicity takes place in a multifractal-like region and not in the entire phase space (or in a nonzero Lebesgue measure of it). Furthermore, it should be mentioned that the results $q_p \neq q_E$ could be due to finite-size effects, but this point deserves further investigation. Indeed, the plethora of results pointing out in many systems the existence of q -triplets and related structures [38,39] could in principle emerge here as well, thus leading to values of q 's that differ among them for different basic quantities. These values could satisfy relations among them which would leave only a small number as independent ones, being all the others functions of those few.

To check the q -Gaussian fits in the one-particle momentum distribution, we used the q -kurtosis [10],

$$\kappa_q(q) \equiv \frac{1}{3} \frac{\langle p^4 \rangle_{2q-1}}{\langle p^2 \rangle_q^2} = \frac{3-q}{1+q}, \quad (5)$$

whereas for the energies, we used the q -ratio [36]

$$\rho_q(q) \equiv \frac{1}{2} \frac{\langle \epsilon^2 \rangle_{2q-1}}{\langle \epsilon \rangle_q^2} = 2 - q, \quad (6)$$

the q -moments being defined as [10,28,29]

$$\langle x^m \rangle_{f(q)} = \frac{\int dx x^m [P(x)]^{f(q)}}{\int dx [P(x)]^{f(q)}} [f(q) \equiv 1 + m(q-1)], \quad (7)$$

with $x = p^2$ ($x = \epsilon$) for eq. (5) (eq. (6)). From the momentum and energy histograms we have computed $\kappa_{q_p}(q_p)$ and $\rho_{q_E}(q_E)$ for several values of α/d : see insets of figs. 2(a), (b). These numerical data exhibit good agreement with the above analytical results. Naturally, neither numerical nor experimental results will ever produce

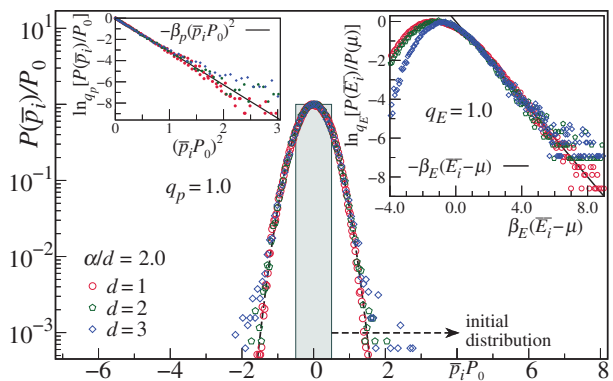


Fig. 3: Distributions for time-averaged momenta \bar{p}_i and energies \bar{E}_i are shown for $\alpha/d = 2$ ($d = 1, 2, 3$). For the momenta we have used conveniently scaled variables (like in fig. 1(a)), and the full line is the Maxwellian ($q = 1$); the left inset shows the same data in a logarithm vs. squared-momentum representation. The right inset exhibits $\ln[P(\bar{E}_i)/P(\mu)]$ vs. $\beta_E(\bar{E}_i - \mu)$. Similarly to fig. 1(b), we verify the appearance of d -dependent densities of states; the full line is an exponential in the variable $\beta_E(\bar{E}_i - \mu)$.

mathematical proofs of whatever analytical expressions of any theory. Interesting illustrations of this trivial fact have been discussed some years ago for compact-support numerical distributions [40,41]. Let us however emphasize that, in the present case, we are focusing on fat-tailed distributions on which such numerical coincidences certainly are much harder to occur along many decades.

For completeness, in fig. 3 we present distributions for time-averaged momenta \bar{p}_i and energies \bar{E}_i , for the short-range-interaction regime $\alpha/d = 2$ ($d = 1, 2, 3$). For the momenta, our data are well fitted by a Gaussian, whereas for the energies one notices a straight line for $\bar{E}_i > \mu$ (see right inset), landmark of the Boltzmann weight. For $\alpha/d = 2$, the lattice dimensionality starts playing an important role, clearly detected in the

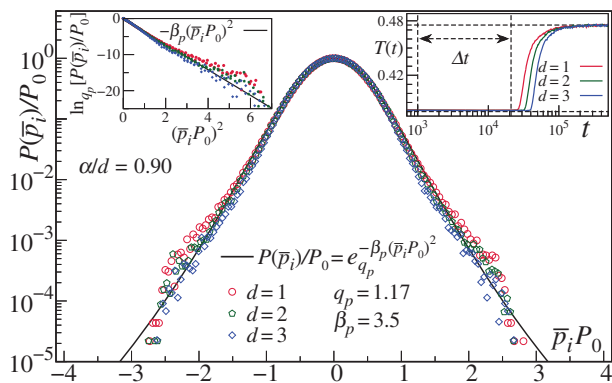


Fig. 4: (Colour online) Distributions of time-averaged momenta \bar{p}_i for the same parameters used in fig. 1(a), but for a different time window. The left inset presents the same data in a q -logarithm vs. squared-momentum representation; the full straight line is a q -Gaussian with $q = 1.17$. One should notice the collapse of all dimensions with nearly the same value of q . The right inset shows $T(t) \equiv 2K(t)/N$ and the time window Δt along which the time averages were calculated ($t \in [1, 21] \times 10^3$).

numerical simulations: i) different dimensions are characterized by distinct density of states, so that the collapse of the energy distributions only occurs for $\bar{E}_i > \mu$; ii) the number of nearest-neighbor rotators increases with d , which directly reflects on the computational time of the simulations (for this reason, we have considered $N = 262144$ for $d = 1$, and $N = 46656$ for $d = 2, 3$).

In fig. 4 we present distributions of momenta for the same systems considered in fig. 1(a), but now for a substantially earlier time window ($t \in [1, 21] \times 10^3$), within the QSS. Once again, the collapse of all three histograms ($d = 1, 2, 3$) into a single q -Gaussian is observed, although for a smaller value, $q_p = 1.17$. The duration t_{QSS} of such a QSS increases with N and decreases with α/d [1,8,10,16]; we verified that $t_{\text{QSS}} \sim N^{\gamma(\alpha/d)}$ with $\gamma(0.9) \simeq 0.6$. Therefore, the analysis of histograms in the QSS must take into account the window Δt for the time averages, according to N and α/d . A detailed study of these effects is out of our present scope and represents a matter for future investigations.

To summarize, we have presented molecular-dynamics results for a classical inertial XY model, on d -dimensional lattices ($d = 1, 2, 3$), characterized by interactions with a variable range. These interactions decay with the distance r_{ij} between rotators at sites i and j , like $1/r_{ij}^\alpha$ ($\alpha \geq 0$), so that, by increasing gradually the parameter α , one interpolates between the infinite-range-interaction ($\alpha = 0$) and the nearest-neighbor ($\alpha \rightarrow \infty$) limits. Our numerical analyses strongly suggest that crucial properties, like probability distributions, depend on the ratio α/d , rather than on α and d separately. For sufficiently high values of α/d we have found Maxwellians for the momenta, as well as the Boltzmann weight for the energies. On the other hand, in the long-range-interaction regime ($\alpha/d < 1$), we have observed q -Gaussians for the

time-averaged momenta, as well as q -exponential distributions for the time-averaged energies, thus undoubtedly falling out of the scope of Boltzmann-Gibbs statistical mechanics. The present study corroborates investigations on different long-range systems, such as the extended Fermi-Pasta-Ulam model and complex networks, thus showing that central properties depend on the ratio α/d . In particular, the values of the indices q herein found vary as $q = q(\alpha/d)$, in full agreement with the theoretical expectations of nonextensive statistical mechanics.

We acknowledge useful conversations with D. BAGCHI, E. P. BORGES, T. BOUNTIS, H. CHRISTODOULIDI, E. M. F. CURADO, G. RUIZ, A. M. C. SOUZA, and U. TIRNAKLI. We benefited from partial financial support by CNPq, FAPERJ, and CAPES (Brazilian agencies), and the John Templeton Foundation (USA).

REFERENCES

- [1] CAMPA A., DAUXOIS T. and RUFFO S., *Phys. Rep.*, **480** (2009) 57.
- [2] LYNDEN-BELL D., *Mon. Not. R. Astron. Soc.*, **136** (1967) 101; LYNDEN-BELL D. and WOOD R., *Mon. Not. R. Astron. Soc.*, **138** (1968) 495.
- [3] JUND P., KIM S. G. and TSALLIS C., *Phys. Rev. B*, **52** (1995) 50.
- [4] TSALLIS C., *Fractals*, **03** (1995) 541.
- [5] DE VEGA H. J. and SÁNCHEZ N., *Nucl. Phys. B*, **625** (2002) 409.
- [6] ANTENEODO C. and TSALLIS C., *Phys. Rev. Lett.*, **80** (1998) 5313.
- [7] BAGCHI D. and TSALLIS C., *Phys. Rev. E*, **93** (2016) 062213.
- [8] BACHELARD R. and KASTNER M., *Phys. Rev. Lett.*, **110** (2013) 170603.
- [9] CIRTO L. J. L., LIMA L. S. and NOBRE F. D., *J. Stat. Mech.: Theory Exp.*, **2015** (2015) P04012.
- [10] CIRTO L. J. L., ASSIS V. R. V. and TSALLIS C., *Physica A*, **393** (2014) 286.
- [11] CHRISTODOULIDI H., TSALLIS C. and BOUNTIS T., *EPL*, **108** (2014) 40006.
- [12] CHRISTODOULIDI H., BOUNTIS T., TSALLIS C. and DROSSOS L., *J. Stat. Mech.: Theory Exp.*, **2016** (2016) 123206.
- [13] LUIJTEN E. and BLÖTE H. W. J., *Phys. Rev. Lett.*, **89** (2002) 025703.
- [14] ANTONI M. and RUFFO S., *Phys. Rev. E*, **52** (1995) 2361.
- [15] PLUCHINO A., RAPISARDA A. and TSALLIS C., *EPL*, **80** (2007) 26002.
- [16] PLUCHINO A., RAPISARDA A. and TSALLIS C., *Physica A*, **387** (2008) 3121.
- [17] TAMARIT F. and ANTENEODO C., *Phys. Rev. Lett.*, **84** (2000) 208.
- [18] CAMPA A., GIANISANTI A. and MORONI D., *J. Phys. A: Math. Gen.*, **36** (2003) 6897.
- [19] BRITO S., DA SILVA L. R. and TSALLIS C., *Sci. Rep.*, **6** (2016) 27992.

- [20] NUNES T. C., BRITO S., DA SILVA L. R. and TSALLIS C., *J. Stat. Mech.: Theory Exp.*, **2017** (2017) 093402.
- [21] GUPTA S. and RUFFO S., *Int. J. Mod. Phys. A*, **32** (2017) 1741018.
- [22] ETTOUMI W. and FIRPO M.-C., *Phys. Rev. E*, **87** (2013) 030102.
- [23] ANTONIAZZI A., FANELLI D., BARRÉ J., CHAVANIS P.-H., DAUXOIS T. and RUFFO S., *Phys. Rev. E*, **75** (2007) 011112.
- [24] ANTONIAZZI A., CALIFANO F., FANELLI D. and RUFFO S., *Phys. Rev. Lett.*, **98** (2007) 150602.
- [25] ANTONIAZZI A., FANELLI D., RUFFO S. and YAMAGUCHI Y. Y., *Phys. Rev. Lett.*, **99** (2007) 040601.
- [26] MARTELLONI G., MARTELLONI G., DE BUYL P. and FANELLI D., *Phys. Rev. E*, **93** (2016) 022107.
- [27] TSALLIS C., *J. Stat. Phys.*, **52** (1988) 479.
- [28] TSALLIS C., MENDES R. S. and PLASTINO A. R., *Physica A*, **261** (1998) 534.
- [29] TSALLIS C., *Introduction to Nonextensive Statistical Mechanics: Approaching a Complex World* (Springer, Berlin) 2009.
- [30] BETZLER A. S. and BORGES E. P., *Mon. Not. R. Astron. Soc.*, **447** (2015) 765.
- [31] TIRNAKLI U. and BORGES E. P., *Sci. Rep.*, **6** (2016) 23644.
- [32] WONG C.-Y., WILK G., CIRTO L. J. L. and TSALLIS C., *Phys. Rev. D*, **91** (2015) 114027.
- [33] YALCIN G. C. and BECK C., *Sci. Rep.*, **8** (2018) 1764.
- [34] YOSHIDA H., *Phys. Lett. A*, **150** (1990) 262; *Celest. Mech. Dyn. Astron.*, **56** (1993) 27.
- [35] HAUKE P. and TAGLIACOZZO L., *Phys. Rev. Lett.*, **111** (2013) 207202.
- [36] BAGCHI D. and TSALLIS C., *Physica A*, **491** (2018) 869.
- [37] RUIZ G., TIRNAKLI U., BORGES E. P. and TSALLIS C., *Phys. Rev. E*, **96** (2017) 042158.
- [38] TSALLIS C., GELL-MANN M. and SATO Y., *Proc. Natl. Acad. Sci. U.S.A.*, **102** (2005) 15377.
- [39] TSALLIS C., *Eur. Phys. J. ST*, **226** (2017) 455.
- [40] HILHORST H. J. and SCHEHR G., *J. Stat. Mech.: Theory Exp.*, **2007** (2007) P06003.
- [41] RODRÍGUEZ A., SCHWÄMMLE V. and TSALLIS C., *J. Stat. Mech.: Theory Exp.*, **2008** (2008) P09006.